Magnetic Nanoparticles Encapsulated in Hydrogel as Hyperthermic Actuators for Microrobots Designed to Operate in the Vascular Network

Seyed Nasr Tabatabaei, Jacinthe Lapointe and Sylvain Martel, *Senior Member, IEEE*

***Abstract*—Our group demonstrated that magnetic nanoparticles such as superparamagnetic iron oxide (Fe_3O_4) when embedded in microrobots, can be used for propulsion and tracking in the human vascular network using an MRI platform. Here, we show that the same magnetic nanoparticles can also be exploited to perform as hyperthermic actuators. More specifically, we show that when embedded in N-isopropylacrylamide (NIPA) thermo responsive hydrogel, vascular microrobots capable of changing their size to adapt to various diameters of blood vessels could be synthesized. This type of hydrogel is not only able to reduce size in response to temperature elevations but it can also be used to release possible therapeutic agents previously trapped within the hydrogel. Here, NIPA hydrogel samples were placed inside an alternating magnetic field of 116 Oe at 145 kHz. Temperature elevations as well as change in hydrogel volume were recorded.**

I. INTRODUCTION

Nowadays researchers around the world have given a significant attention to hyperthermia via elevation of target tissue temperature by dissipation of heat from Magnetic NanoParticles (MNP) placed in an external time-varying magnetic field. However the complexity of such approach in fight against malignant cells in a physiological system causes it to be an extremely challenging task. This is caused by numerous parameters that differently affect the final change in tissue temperature, for instance, alteration in smallest physical and/or biological condition of the subject at study. There is no doubt however, that MNP have the potential to be the key medical nanorobots to diagnose and treat cancerous tissues. Their controllable size allows them to bond and interact with biological entity of interest such as cell (10-100 µm), virus (20-450 nm), protein (5-50 nm) or gene (2 nm wide, 10-100 nm long) once they are coated with biodegradable and biocompatible molecules such as dextran, polyvinyl alcohol and phospholipids [1]. These magnetic nanorobots can also be propelled through blood vessels with the help of an external magnetic gradient field.

Manuscript received March 1, 2009. This project is supported in part by a Canada Research Chair (CRC) in Micro/Nanosystem Development, Fabrication and Validation, the Canada Foundation for Innovation (CFI), the National Sciences and Engineering Research Council of Canada (NSERC), and the Fonds Québécois de Recherche sur la Nature et les Technologies (FQRNT).

Seyed Nasr. Tabatabaei is with NanoRobotics Laboratory, Ecole Polytechnique de Montreal, QC, H3T 1J4 Canada (phone: 514-340-4711 ext: 5029; fax: 514-340-5280; e-mail: nasr.tabatabaei@polymtl.ca).

Jacinthe Lapointe is with NanoRobotics Laboratory, Ecole Polytechnique de Montreal, QC, H3T 1J4 Canada. (e-mail: jacinthe.lapointe@polymtl.ca).

Sylvain Martel (corresponding author) is director of NanoRobotics Laboratory, École Polytechnique de Montréal, QC, Canada H3T 1J4 (e-mail: sylvain.martel@polymtl.ca).

An interesting recent subject hence the topic of this paper is hyperthermic-based functionality of MNP for trigger a drug-release mechanism using hydrogel carriers. Hydrogels are polymers that are able to absorb large quantities of water without dissolving or losing their tridimensional structure. They are used in biomedical application because of their physical properties similar to those of living tissue and their high level of biocompatibility. Some hydrogels are known as "smart" gels due to their response to an external stimulus such as change in temperature, pH, magnetic fields, etc. In this study thermo-responsive hydrogel is of interest in which N-isopropylacrylamide (NIPA) hydrogel is the most familiar type. This type of hydrogel is able to reduce size in response to temperature elevation, a sponge like quality that can be used to assist release of therapeutic agents embedded within the gel at adjustable desired temperature [2]. What assists elevation of hydrogel temperature in this case is MNP embedded within the gel. Once hydrogel with embedded MNP are placed in an alternating magnetic field, the energy from the magnetic field is dissipated to heat and then transferred from MNP to the hydrogel thus increasing its temperature.

Therefore the final goal is to integrate MNP with therapeutic agents in micro-carriers made of NIPA hydrogel that are capable of transiting through the smallest capillaries. These micro-carriers can be navigated towards a target such as a tumor using a method similar to the one described in [3] where a 1.5 mm ferromagnetic bead was navigated in the carotid artery of a living swine. Instead of a large magnetic core to guide mentioned micro-carriers in capillaries, the proposed hydrogel micro-carriers can rely on an agglomeration of – embedded within hydrogel – contrast agents MNP used also for propulsion through an induction of magnetic gradients generated by a clinical MRI system. This allows tracking of the micro-carriers as local distortion of the magnetic field inside the MRI system where the confirmation of homogenous distribution of micro-carriers at the target area prior to drug release is easily feasible [4]. Once micro-carriers are aggregated around target area by means of embolization, AC magnetic field can cause embedded MNP to heat the NIPA hydrogel micro-carriers and as a consequence actuate a drug release sequence. At this time, as a result of reduction in hydrogel micro-carrier volume a fraction of embedded MNP along with therapeutic agents are liberated allowing the micro-carrier to move closer towards the target area. Also released MNP around the target area can proceed further in the capillaries and attach to the target tissue by means of antibodies. This may change the topography cues of the environment and neighboring cells and may influence cell cytoskeleton

formation. The resulting nano-bumps and nano-spheres on target cells can encourage the cells to switch from growth to apoptosis – cell's self destruction mechanism [5].

II. Materials and Methods

A. Magnetic Loss

The heat generated by MNP placed in an AC magnetic field is mainly caused by three major mechanisms; hysteresis loss, Néel and Brownian relaxation. Among these depending on the particle size, shape, composition, concentration and viscosity of the suspended medium as well as magnitude and frequency of the applied magnetic field, one is dominant. The power which participates in generation of heat per gram of the magnetic material is calculated using calorimetric measurements and is referred to as specific absorption rate (SAR) or specific loss power (SLP).

i. Multi-domain Magnetic Nanoparticles

Large ferromagnetic materials above approximately 80 nm [6] consist of several magnetic domains. Each domain contains large numbers of atomic magnetic moments, m, caused by current generated due to spin of the electrons. These moments are aligned parallel below a critical temperature to lower the exchange energy. According to Weiss domain theory [7], the direction of the aligned moments varies randomly from domain to domain and in the absence of a magnetic field this direction is aligned along magnetic crystallographic axes called 'easy axes'. The energy required to overcome the resistive force against any attempt by magnetic field to rotate domain directions is called anisotropy energy, $E = KV$, where K is the effective anisotropy constant and V is the volume of the magnetic core [8], [9]. When multi-domain material in its demagnetized state is subject to a low external magnetic field H, domains with magnetic moments aligned favorably with respect to the magnetic field direction grow in size and those opposing it reduce in size. As magnetic field energy is increased, magnetic moments overcome the anisotropy energy and rotate into a new set of magnetic crystallographic axes nearest to field direction. Finally, further increase in magnetic field amplitude leads to magnetization saturation M_S of the magnetic moments and a gradual alignment along the magnetic field direction [7]. The magnetization however can be reduced to zero by applying a magnetic field of strength in the opposite direction. However magnetization curves for increasing and decreasing magnetic field amplitudes do not coincide. Therefore the material demonstrates "hysteresis behavior" and hysteresis losses are expressed in form of heat transferred to the surrounding medium. Mathematically SAR is proportional to the product of frequency and the integral of the hysteresis loop [10]. In other words the wider the area under the loop, the more heat is dissipated to the surrounding area.

ii. Single-domain Magnetic Nanoparticles

In case of fine ferromagnetic single domain particles with hexagonal (uniaxial) anisotropy such as cobalt, when the difference between the maximum and minimum energy per unit volume – set by anisotropy energy – of the particle is larger than its thermal energy kT, where k is Boltzmann constant, thermal agitation is ignored and static magnetization curve calculated by Stoner-Wohlfarth [11] will lead to narrow hysteresis. In single domain particles this behavior and consequently energy released as heat can be better explained by Néel relaxation mechanism. As in multi-domain particles, when the external magnetic field amplitude is larger than the anisotropy field

$$H_{anisotropy} = 2K / \mu_0 M_s \quad (1)$$

where M_s is the magnetization saturation, the anisotropy energy barrier is overcome and magnetic moments will rotate onto the anisotropy axis closest to the external magnetic field direction. If this field is increased further, magnetic moments will then gradually align along the magnetic field direction and reach saturation state. Once the external magnetic field is removed however, magnetic moments take certain time equivalent to Néel relaxation time τ_N to relax and rotate back to their equilibrium orientation (easy axes) [12].

The third mechanism is Brownian relaxation that causes both multi-domain and single domain particles to heat up. In this case energy barrier for reorientation of a particle is given by rotational friction due to the rotation of the entire magnetic particle caused by the AC magnetic field torque force on the magnetic moment of the particle. The viscosity of the medium that the particles are suspended in as well as their hydrodynamic volume has a direct effect on Brownian relaxation time, τ_B, which is defined as the time the particle takes to rotate while influenced by the external magnetic field. In our case since the MNP are embedded inside hydrogel, Brownian relaxation has negligible effect on total value of SAR.

iii. Superparamagnetism

In smaller single domain magnetic particles called superparamagnetic particles – less than 20 nm in diameter for Iron Oxide (Fe_3O_4) MNP [14] – the difference between the maximum and minimum values of the particle energy per unit volume is much smaller than kT. The orientation of the magnetic moment of these particles therefore continuously changes due to thermal agitation. For an aggregation of such particles this fluctuation leads to 'conservation of distribution orientations characteristic of statistical equilibrium' [15]. Therefore hysteresis losses cannot occur. In other words, thermal energy becomes significant enough to cause magnetic moments random fluctuation in the absence of external magnetic field energy. However in this case, if the applied magnetic field is large enough, the energy from the field drives magnetic moments to rotate and aligns them along the magnetic field direction by overcoming the thermal energy barrier. Once the external magnetic field is removed, magnetic moments do not relax immediately, they rather take τ_N seconds to randomize their direction to their original orientation at the presence of thermal energy. The relation between magnetization and applied magnetic field is expressed by a parameter called magnetic susceptibility χ through the formula

$$M = \chi H \quad (2)$$

This parameter explains how magnetization varies with applied magnetic field. When superparamagnetic nanoparticles are subjected to an alternating magnetic field, the loss is not due to hysteresis behavior but rather from the fact that magnetization lags the applied magnetic field. This phenomenon is simulated mathematically using complex magnetic susceptibility. For an alternating applied magnetic field

$$H(t) = H_0 \cos(\omega t) \quad (3)$$

complex susceptibility is represented by

$$\chi = \chi' - i\,\chi'' \quad (4)$$

which leads to magnetization of

$$M(t) = H_0 (\chi' \cos(\omega t) + \chi'' \sin(\omega t)) \quad (5)$$

The imaginary part χ'' in (5) is due the phase difference between the applied magnetic field and corresponding magnetization which is why it is responsible for heat dissipation [16].

B. *Iron Oxide Superparamagnetic Nanoparticles*

In a biological system, to minimize the amount of magnetic material dosage it is advantageous to obtain the highest value for SAR. However there are biological, technical and economical limitations to this approach. To respect both limitations as well as maximizing SAR, superparamagnetic nanoparticles have shown impressive potential.

Previously we mentioned that dissipated heat from multi-domain MNP is calculated from frequency multiplied by the area of the hysteresis loop. To benefit from maximum hysteresis loop, particles have to magnetically saturate to extremely high fields in the orders of few thousands of Oersted. Such fields may cause unwanted tissue heating, stimulation of peripheral and skeletal muscles and irreversible biological effects such as cardiac fibrillation [17]. Therefore adequate magnetic field and frequency that is required to make use of the entire hysteresis loop is too high to consider for hyperthermia. In addition, because multi-domain MNP ensemble align randomly with the magnetic field, only 25% of the ideal maximum calculated power may be dissipated as heat [18]. It is observed however that substantial heat can be produced by using superparamagnetic nanoparticles up to three times that of multi-domain MNP thanks to their susceptibility and magnetic relaxation mechanisms [19].

i. *Physical and Chemical Properties*

Commercially available superparamagnetic iron oxide nanoparticles coated with dextran (Product number: 79-00-201, micromod, Germany) and suspended uniformly in water were purchased. Transmission electron microscopy (TEM: Jeol JEM-2100F) measurements confirmed the crystal structure (Fe_3O_4) and it also revealed the narrow diameter distribution size to be 7-10 nm (Figure 1a).

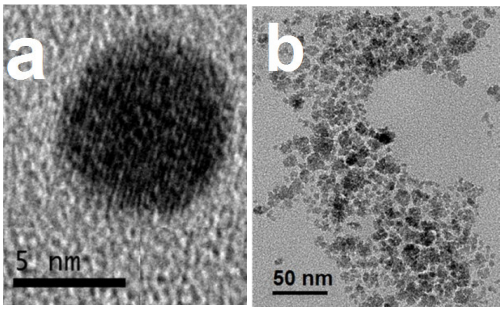

Fig. 1a. TEM image of a single domain Iron Oxide MNP
Fig. 1b. Agglomeration of the iron oxide MNP in the solution.

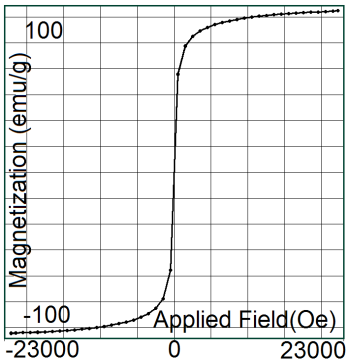

Fig. 2. Lack of hysteresis curve of MNP obtained by VSM measurements indicates superparamagnetic behavior of our Iron Oxide MNP.

Hydrodynamic mean diameter was measured to be 58.77 nm by analysis of photon correlation spectroscopic analyzer (PCS: Malvem Instruments Ltd.). This difference in diameter is explained by agglomeration of the particles (Figure 1b) caused by Van der Waals forces, Brownian motion and intermolecular cohesive forces acting on immersed MNP in the solution [20] in addition to dextran mass that was verified to be as high as 50% of total mass of the particle by the atomic absorption spectrometry (AAS: Thermo Scientific S Series). Lack of hysteresis curve measured by vibrating sample magnetometer (VSM: EV5, Magnetics) verified superparamagnetic nature of the iron oxide MNP shown in Figure 2. In this experiment MNP were divided into two pairs of 5 and 12.5 mg Fe/ml by means of distillation from the initial 5 mg Fe/ml solution.

ii. *Magnetic Field Parameter*

Frequency of the magnetic field in this study was estimated to be 145 kHz using calculated spectra for the imaginary part of the susceptibility for immobilized particles shown by Hergt *et al*. [21]. This estimation also agrees with his previous work [22] where loss power due to Néel relaxation reached maximum for MNP of 10 nm in diameter at frequencies less than 200 kHz.

In other hand, magnetic field strength was obtained dealing with biological limitations with the derivative of magnetic flux density over time. Although limitations to occupational and general public exposure to AC magnetic field are much lower than those of medical [17], in a study

involving electromyography recording of human arm [23], it was observed that a derivative of AC magnetic flux density dB/dt greater than 10^4 T s^{-1} was required to stimulate the median nerve trunk. Mathematical simulation of dB/dt assured that maximum 10^4 T s^{-1} limit can be avoided for a magnetic field strength equal to 116 Oe at 145 kHz. This simulation also took into account values for biological tissue conductivity ranging from 0.0144 S.m^{-1} to 0.68 S. m^{-1} as tabulated in [24] for frequencies in the range of 100 kHz.

C. N-isopropylacrylamide (NIPA) Hydrogel

NIPA has an inverse response to temperature elevation, that is, it reduces size when heated and swells when cooled down. This discontinuous and reversible mechanism caused by internal structure changes due to the presence of hydrophobic groups occurs at lower critical solution temperature (LCST). At temperatures below LCST, hydrogen bonds between hydrophilic groups of polymer chain are dominant, i.e. dissolution of water has increased. When temperature is increased to LCST, hydrogen bonds become weak and hydrophobic interaction become stronger, which results in shrinking of the hydrogel. The LCST of PNIPA hydrogel alone is at 32 °C, and can be set above body temperature by copolymerization with hydrophobic monomer like acrylic acid [25], [26]. In our case, LCST for MNP embedded NIPA hydrogel was determined to be 29 °C. The interaction between MNP and/or their polymer coating with the hydrogel may have had an effect on reduction of LCST.

D. Chemical Synthesis

i. Hydrogel

The hydrogel is synthesized by free-radical chain polymerization, which is the addition of monomer unit to a growing polymer chain. The reaction has to be initiated by a product that will create a radical. That radical will be added to the first monomer of the chain. In our case, the monomer is N-isopropylacrylamide (NIPA) and the initiator is ammonium persulfate (APS). N,N,N',N'-tetramethylenediamine (TEMED) is also used as an accelerator for this reaction. The presence of the cross-linker, the N,N-methylene(bis)acrylamide (BIS) helps in solidification and creation of the gel [27].

The hydrogel was prepared by dissolving 7.5 mmol of the NIPA, 0.075 mmol of BIS and 0.075 mmol of TEMED in 6 ml of water. The solution was bubbled with nitrogen for 10 minutes to remove the residual oxygen, which has a detrimental effect on polymerization. Then 0.6 ml of this solution was added to 0.4 ml of Fe_3O_4 superparamagnetic nanoparticles to get 1 ml final volume. Finally, 0.001 mmol of initiator (APS) was added (3.4 µl of a 10% wt solution) to start the polymerization process. The time needed to complete the polymerization process was 24 hours at room temperature [2], [28]. Two sets of samples were synthesized with the two concentrations of Fe_3O_4 superparamagnetic nanoparticles. Final hydrogel solutions contained 0.5 ml of 1 mgFe/ml and 5 mgFe/ml. A third set of 0.5 ml hydrogel samples with no MNP were prepared as control set. Samples were placed inside cylindrical plastic containers with 10.5 mm in diameter and 40.3 mm in height.

ii. Agar gel

For this experiment, we tested hydrogel temperature response to magnetic field inside both insulation styrofoam and 5% w/v Agar gel to simulate microstructures in hard tissue conditions. To create Agar gel, 10 grams of Agar powder (DIFCO Laboratories) was added to 200 ml distilled water. The solution was stirred and heated to 80 °C for 30 minutes and then left to cool down to room temperature for an hour. The final gel was cut to fit inside induction coil. A hole was then made in the middle of the Agar to shape the plastic sample container.

E. Experimental Setup

For the first part of this experiment (Figure 3), sample containers were carefully placed in the center of the Agar gel so that NIPA hydrogel inside the sample was buried below Agar surface. Agar gel was put in the middle and inside a 3 turn costume made copper tube coil with 67 mm in diameter. The coil was powered by an induction machine (2kW HotShot, Ameritherm Inc,) generating a magnetic field equivalent to 116 Oe at 145 kHz.

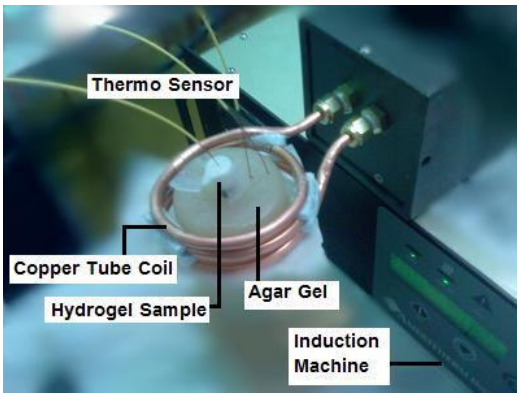

Fig. 3. Induction of hydrogel sample in Agar gel.

Temperatures of the NIPA hydrogel and surrounding area up to 10 mm away from the center of Agar gel were recorded by fiber optic temperature sensors (Reflex, SN: T18 217A, Neoptix Inc, QC, Canada). The induction machine was turned on 10 seconds after starting time for temperature recording and turned off in 30 minute interval for each sample.

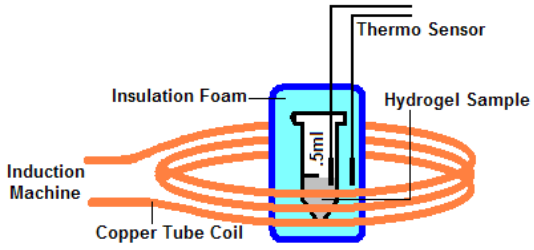

Fig. 4. Schematics of induction of hydrogel sample in insulation styrofoam.

Second part of this experiment (Figure 4) consisted of insulation styrofoam instead of the Agar gel. The sample containers were placed in the cylindrical styrofoam (The Dow Chemical Co.) with 27 mm in diameter and 45 mm in

height such that the NIPA hydrogel was completely covered inside styrofoam. The styrofoam was then placed at the center of the copper tube coil and temperature changes were recorded via fiber optic temperature sensors.

Finally a 20 mm^3 NIPA hydrogel containing 5 mgFe/ml of MNP was placed inside a channel fabricated on PMMA (Figure 5). The NIPA hydrogel was then heated on a hot plate to 29 °C. Temperature readings were taken by an infrared thermometer (Oakton, TempTestr IR) and the effect of heat on volume was observed by a microscope.

III. Results

Tabulated results are shown in Table 1 and 2 where initial and final temperatures as well as temperature differences for each sample are presented. More detailed scope of the results are shown for samples placed in Agar and in insulation styrofoam in Figure 6 and 7 respectively. Remarkable changes of volume in samples containing 5 mgFe/ml NIPA after reaching 29 °C were observed. For these samples the dark red color of NIPA hydrogel (Figure 5a) turned gray (Figure 5d) and the volume decreased substantially to less than 12 mm^3. Within hours of cooling these samples gained most of their original volume ready to be re-heated.

Table 1
Temperature changes for samples inside Agar gel

AGAR	T 1(°C) t = 0 s	T 2(°C) t = 1810 s	T2-T1
Hydrogel	17.1	18.5	1.4
Surrounding	17.1	18.8	1.7
1 mgFe/ml NIPA	18.1	21.1	3
Surrounding	17.8	20.1	2.3
5 mgFe/ml NIPA	18.5	21.8	3.3
Surrounding	18.3	20.9	2.6

Table 2
Temperature changes for samples inside styrofoam insulation

STYROFOAM	T 1(°C) t = 0 s	T 2(°C) t = 1810 s	T2-T1
Hydrogel	25.6	25.8	0.2
Surrounding	25.8	26.1	0.3
1 mgFe/ml NIPA	25.6	27.7	2.1
Surrounding	25.6	27.1	1.5
5 mgFe/ml NIPA	24.7	29.1	4.4
Surrounding	25.3	27.8	2.5

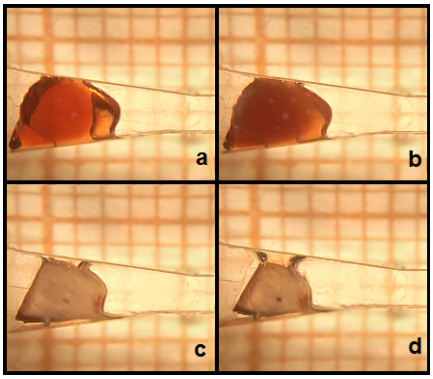

Fig. 5. Remarkable volume reduction (a-d) of 20 mm^3 5 mgFe/ml NIPA hydrogel when heated to 29 °C to less than 12 mm^3.

IV. Discussion

In the region of the magnetic field, it is reasonable to assume uniformity of the field due to small distribution size of MNP compared to the coil dimensions. Also the samples were positioned in the middle of the field where the field is most uniform. Therefore the variation of the magnetic field is expected to be minimal. At fixed frequency and applied magnetic field, hydrogel samples containing MNP reached a stabilized temperature level. This can be explained by thermodynamic equilibrium effect taking place between heating source and the surrounding area. Another possible explanation may be thermal energy effects on the magnetic degradation of iron oxide MNP; as ambient temperature is increased by the magnetic field, spin damping or decrease in magnetic moment of MNP as well as decrease in anisotropy constant causes a reduction in the amount of magnetically induced heat generation and reduces total loss [8], [10].

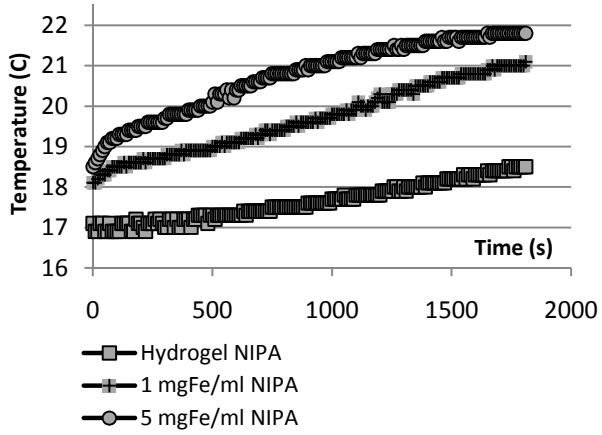

Fig. 6. Temperature change versus time for two samples of hydrogel embedded MNP inside *Agar gel* and hydrogel control sample.

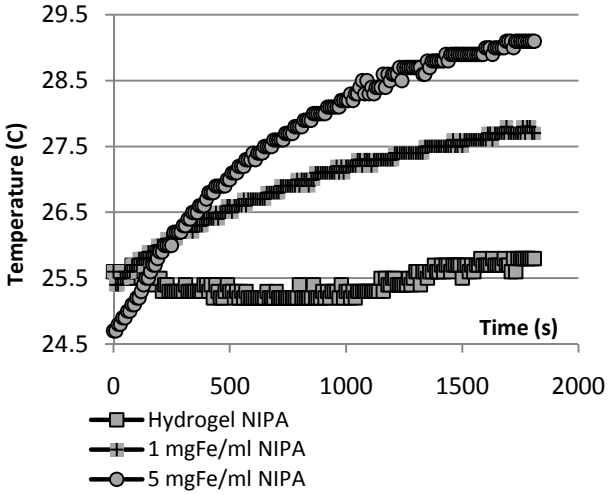

Fig. 7. Temperature change versus time for two samples of hydrogel embedded MNP inside *styrofoam insulation* and hydrogel control sample.

The Agar gel initial temperature was at 17 °C, more than 6 °C below room temperature. This may be due to constant liquid evaporation of the Agar material at room temperature. However this low temperature allowed elevation of

temperature no more than 3.3 °C for NIPA hydrogel with highest concentration of iron oxide MNP. Magnetic field had little effect on hydrogel NIPA samples without any MNP inside. The 1 °C elevation of temperature could be result of Eddy currents that are generated by the induction machine. However these currents are neglected in SAR calculations due to small size of MNP compare to the coil dimentions. Once the samples were placed in insulation styrofoam at room temperature, it was evident that higher concentration of iron oxide MNP trapped in NIPA hydrogel have higher rate of heat. As seen in Table 2, these samples reached their LCST value in 30 minutes.

V. Conclusion

In this paper we showed a method of synthesizing NIPA hydrogel mixed with iron oxide superparamagnetic nanoparticles to enhance the capability of microrobots. We demonstrated experimentally in previous papers that MNP alone can be used with an MRI system to propel and track microrobots in the vascular network. By embedding MNP in future hydrogel-based microrobots, the dimensions of the robots could be changed when required to travel through various blood vessel diameters. Such mixture of MNP with hydrogel could also provide a method for such microrobots to anchor at specific locations by volumetric expansion. Additional functionality could also be implemented such as temporary embolization and triggered drug releases for therapeutic microrobots.

References

[1] Q. A. Pankhurst, "Nanomagnetic medical sensors and treatment methodologies," *BT Technology Journal*, vol. 24, pp. 33-38, 2006.

[2] K. L. Ang, S. Venkatraman, and R. V. Ramanujan, "Magnetic PNIPA hydrogels for hyperthermia applications in cancer therapy," *Materials Science and Engineering: C*, vol. 27, pp. 347-351, 2007.

[3] S. Martel, J.-B. Mathieu, O. Felfoul, A. Chanu, E. Aboussouan, S. Tamaz, P. Pouponneau, L. H. Yahia, G. Beaudoin, G. Soulez, and M. Mankiewicz, "Automatic navigation of an untethered device in the artery of a living animal using a conventional clinical magnetic resonance imaging system," *Applied Physics Letters*, vol. 90, pp. 114105, 2007.

[4] Ste´phane Mornet, Se´bastien Vasseur, F. G. and, and E. Duguet, "Magnetic nanoparticle design for medical diagnosis and therapy," *Materials Chemistry*, vol. 14, pp. 2161-2175, 2004.

[5] C. C. Berry and A. S. G. Curtis, "Functionalisation of magnetic nanoparticles for applications in biomedicine," *Journal of Physics D: Applied Physics*, vol. 36, pp. 198-206, 2003.

[6] R. F. Butler and S. K. Banerjee, "Theoretical Single-Domain Grain Size Range in Magnetite and Titanomagnetite," *J. Geophys. Res.*, vol. 80.

[7] D. Jiles, *Introduction to magnetism and magnetic materials*, 1st ed. New York: Chapman and Hall, 1990.

[8] C. Benard Dennis, *Introduction to magnetic materials*. New York: Addison-Wesley, 1972.

[9] E. Duguet, S. Vasseur, S. Mornet, G. Goglio, A. Demourgues, J. Portier, F. Grasset, P. Veverka, and E. Pollert, "Towards a versatile platform based on magnetic nanoparticles for in vivo applications," *Bulletin of Materials Science*, vol. 29, pp. 581-6, 2006.

[10] S. Bae, S. W. Lee, Y. Takemura, E. Yamashita, J. Kunisaki, S. Zurn, and C. S. Kim, "Dependence of frequency and magnetic field on self-heating characteristics of NiFe2O4 nanoparticles for hyperthermia," *IEEE Transactions on Magnetics*, vol. 42, pp. 3566-3568, 2006.

[11] E. C. Stoner and E. P. Wohlfarth, "A mechanism of magnetic hysteresis in heterogeneous alloys," *Magnetics, IEEE Transactions on*, vol. 27, pp. 3475-3518, 1991.

[12] W. F. Brown, "Thermal Fluctuations of a Single-Domain Particle," *Physical Review*, vol. 130, pp. 1677, 1963.

[13] D. Weller and A. Moser, "Thermal effect limits in ultrahigh density magnetic recording," *IEEE Transactions on Magnetics*, vol. 35, pp. 4423-4439, November 1999.

[14] Mi Kyong Yoo, In Yong Kim, Eun Mi Kim, Hwan-Jeong Jeong, Chang-Moon Lee, Yong Yeon Jeong, Toshihiro Akaike, and C. S. Cho, "Superparamagnetic Iron Oxide Nanoparticles Coated with Galactose-Carrying Polymer for Hepatocyte Targeting," *Journal of Biomedicine and Biotechnology*, vol. 2007, 2007.

[15] Brown and W. Fuller, "Thermal Fluctuations of a Single-Domain Particle," *Physical Review*, vol. 130, pp. 1677, 1963.

[16] R. E. Rosensweig, "Heating magnetic fluid with alternating magnetic field," *Journal of Magnetism and Magnetic Materials*, vol. 252, pp. 370-374, 2002.

[17] ICNIRP, "Guidelines for limiting exposure to time-varying electric, magnetic, and electromagnetic fields (up to 300 GHz)," *Health Physics*, vol. 74, pp. 494-522, 1998.

[18] Q. A. Pankhurst, J. Connolly, S. K. Jones, and J. Dobson, "Applications of magnetic nanoparticles in biomedicine," *Journal of Physics D: Applied Physics*, vol. 36, pp. R167-R181, 2003.

[19] J. Arora, "AC-susceptibility studies of magnetic relaxation mechanisms in superparamagnetic nanoparticles." United States -- Texas: The University of Texas at El Paso, 2007.

[20] A. Sharma, Y. Qiang, D. Meyer, R. Souza, A. McConnaughoy, L. Muldoon, and D. Baer, "Biocompatible core-shell magnetic nanoparticles for cancer treatment," presented at Proceedings of the 52nd Annual Conference on Magnetism and Magnetic Materials, Tampa, Florida (USA), 2008.

[21] R. Hergt, R. Hiergeist, M. Zeisberger, G. Glockl, W. Weitschies, L. P. Ramirez, I. Hilger, and W. A. Kaiser, "Enhancement of AC-losses of magnetic nanoparticles for heating applications," *Journal of Magnetism and Magnetic Materials*, vol. 280, pp. 358-368, 2004.

[22] R. Hergt, W. Andra, C. G. d'Ambly, I. Hilger, W. A. Kaiser, U. Richter, and H. G. Schmidt, "Physical limits of hyperthermia using magnetite fine particles," *Magnetics, IEEE Transactions on*, vol. 34, pp. 3745-3754, 1998.

[23] M. Polson, A. Barker, and I. Freeston, "Stimulation of nerve trunks with time-varying magnetic fields," *Medical and Biological Engineering and Computing*, vol. 20, pp. 243-244, 1982.

[24] E. P. Charles Polk, *Handbook of Biological Effects of Electromagnetic Fields*, 2nd ed: CRC, December 21, 1995.

[25] E. S. GIL and S. M. HUDSON, "STIMULI-REPONSIVE POLYMERS AND THEIR BIOCONJUGATES," *PROGRESS IN POLYMER SCIENCE*, vol. 29, pp. 1173-1222, 2004.

[26] C. SATISH, K. SATISH, and H. SHIVAKUMAR, "HYDROGELS AS CONTROLLED DRUG DELIVERY SYSTEMS: SYNTHESIS, CROSSLINKING, WATER AND DRUG TRANSPORT MECHANISM," *INDIAN JOURNAL OF PHARMACEUTICAL SCIENCES*, vol. 68, pp. 133-140, 2006.

[27] N. Aragrag, D. C. Castiglione, P. R. Davies, F. J. Davis, and S. I. Patel, "General procedures in chain-growth polymerization," in *Polymer chemistry : a practical approach*: Oxford University Press, 2004, pp. 43-98.

[28] P. M. XULU, G. FILIPCSEI, and M. ZRINYI, "PREPARATION AND RESPONSIVE PROPERTIES OF MAGNETICALLY SOFT POLY(N-ISOPROPYLACRYLAMIDE) GELS," *MACROMOLECULES*, vol. 33, pp. 1716-1719, 2000.